

of the monodentate complex (169 ppm), we see that the binding of the free carboxylate to a second $\text{Co}^{\text{III}}(\text{NH}_3)_5$ group determines a further upfield shift on the former carbon atom. If in the present system the second carboxylate of oxalate is bound to a positively charged protein residue whose effect is similar to the binding to a metal ion but smaller, the observed ^{13}C NMR spectra can be accounted for. The signal at 169 pp. would correspond to the protein-bound carbon whereas that at 166 to the metal-bound carbon. In the case of bipovalent metal ions the effect of the metal ion is more similar to that of the protein, and a single signal (although broad) is observed.

The spectrum of the monometal derivative is very helpful in discriminating between the two groups of resonances and allows us a comparison between anion arrangements in the two sites. Group 1 resonances refer to oxalate in the C-terminal site and group 2 to oxalate in the N-terminal site. On the basis of the chemical shift values, anion binding at the two sites appears very similar. Namely, the protein-bound carbon exhibits the same chemical shift value at both sites (so pointing toward an identity of the anion binding ligand(s)) whereas the chemical shift value

of the metal-bound carbon is just slightly different.

Concluding Remarks. Our ^{13}C data support the idea that the synergistic anion is bridging the metal to some positively charged group of the protein in agreement with the interlocking-sites model. The structure of the two carbonate binding sites appears identical within the resolution of the technique. Chemical shift values point toward carbonate as the form of the bound anion.

In the case of oxalate, a close analysis of the spectral data allows us to differentiate between the two sites and to state that the anion arrangement is very similar but not identical in the two protein domains. The results appear relevant as far as the structure-function relations of transferrins are concerned. Oxalate seems to act as a monodentate with the second carboxylate group interacting with positively charged residues of the protein.

Acknowledgment. The 754-MHz ^{13}C NMR spectra have been recorded at the high-field NMR center, CNR, Bologna, Italy. Thanks are expressed to D. Macciantelli for technical assistance. This work has been performed with the contribution of the Progetto Finalizzato del CNR, Chimica Fine e Secondaria.

Contribution from the Department of Chemistry, University of Illinois at Chicago, Chicago, Illinois 60680, Department of Physics, Technische Hogeschool, 5600 MB Eindhoven, The Netherlands, and Laboratoire de Spectrochimie des Elements de Transition, UA 420, Université de Paris Sud, 91405 Orsay, France

Magnetochemistry of Copper(II): Exchange Interactions in Catenated $[\text{Cu}(\text{NH}_3)_2(\text{CH}_3\text{COO})\text{Br}]$

Richard L. Carlin,*^{1a} Klaas Kopinga,^{1b} Olivier Kahn,*^{1c} and Michel Verdaguer^{1c,d}

Received October 7, 1985

The specific heat and susceptibility of polycrystalline samples of $[\text{Cu}(\text{NH}_3)_2(\text{CH}_3\text{COO})\text{Br}]$ have been measured over the respective temperature intervals of 1.5–50 and 1.2–60 K. Long-range antiferromagnetic order is found at $T_c = 4.146$ K. The specific heat data have been analyzed in terms of the Bonner-Fisher model for linear chains with $J/k = -4.3 \pm 0.4$ K; the susceptibility data above 10 K may be fit by the same model and exchange constant, with a large molecular field correction, $zJ'/k = -1.9$ K. With the critical entropy $S_c = 42\%$ and with a zigzag linear-chain structure, the substance exhibits unexpectedly large interchain interactions. The mechanism of intra- and interchain interactions is discussed. This latter phenomenon is attributed to the hydrogen-bonding networks linking the chains together.

Introduction

The acetate ion can provide a strong superexchange path in copper compounds. This is illustrated by the early studies^{2,3} on hydrated copper acetate, $[\text{Cu}(\text{CH}_3\text{COO})_2(\text{H}_2\text{O})_2]_n$, in which the copper ions are bridged symmetrically by four acetate groups. Given the Bleaney-Bowers formulation for the exchange coupling in this molecule, the best value⁴ of the exchange constant is $2J/k = -429$ K. A variety of related molecules are known in which the exchange is also strong.^{5,6} The ability of the carboxylate group to transmit the interaction between two copper(II) ions separated by more than 5 Å was also demonstrated in the case of (μ -oxalato)copper(II) compounds.^{7,8} For instance, in $[\text{tmen}(\text{H}_2\text{O})\text{Cu}(\text{C}_2\text{O}_4)\text{Cu}(\text{H}_2\text{O})\text{tmen}](\text{ClO}_4)_2$, $2J/k$ was found as large as -558 K with a Cu...Cu separation of 5.14 Å.⁷

Copper ions are bridged differently, in a zigzag fashion, by nitrate ions in $\text{Cu}(\text{NO}_3)_2 \cdot 2^{1/2}\text{H}_2\text{O}$.⁹ This leads to an exchange

interaction which is much weaker than that in the case described above. The best-fit analysis¹⁰ of a variety of data on copper nitrate is in terms of an alternating-linear-chain antiferromagnet, with α (the degree of alternation) = 0.27 and $J/k = -2.58$ K. This substance does not order spontaneously.

In light of the above, we were drawn to $[\text{Cu}(\text{NH}_3)_2(\text{CH}_3\text{COO})\text{Br}]$, which has a polymeric structure.¹¹ The acetate ion is in a bridging situation between two copper atoms, so that the structure consists of zigzag chains of coordination polyhedra running parallel to [100]. The Cu–O bond distances of the acetate that bridges two metal ions are the same (1.995 (5), 2.001 (6) Å), but the Cu–O–C–O–Cu superexchange path is not a symmetric one. A sketch of the structure is illustrated in Figure 1. The question asked is as follows: How strong would the exchange be, and what is the nature of its dimensionality?

Experimental Section

The compound was prepared as described by Tomlinson and Hathaway.¹² Slow cooling and evaporation of a warm solution of CuBr_2 (5 g) in ammonia solution (10 mL, $d = 0.88$ g/cm³), acetic acid (7.3 mL), and ethanol (70 mL) result in small needle-shaped blue single crystals within a few hours. The compound was washed with ethanol and ether

(1) (a) University of Illinois at Chicago. (b) Technische Hogeschool Eindhoven. (c) Université de Paris Sud. (d) Permanent address: ENS, Le Parc, 92211 Saint Cloud, France.

(2) Bleaney, B.; Bowers, K. D. *Proc. R. Soc. London, Ser. A* **1952**, *214*, 451.

(3) Figgis, B. N.; Martin, R. L. *J. Chem. Soc.* **1956**, 3837.

(4) Güdel, H. U.; Stebler, A.; Furrer, A. *Inorg. Chem.* **1979**, *18*, 1021.

(5) Carlin, R. L.; van Duijneveldt, A. J. *Magnetic Properties of Transition Metal Compounds*; Springer-Verlag: New York, 1977.

(6) Carlin, R. L. *Magnetochemistry*; Springer-Verlag: West Berlin, Heidelberg, New York, Tokyo, 1986.

(7) Julve, M.; Verdaguer, M.; Gleizes, A.; Philoche-Levisalle, M.; Kahn, O. *Inorg. Chem.* **1984**, *23*, 3808.

(8) Michalowicz, A.; Girerd, J. J.; Goulon, J. *Inorg. Chem.* **1979**, *11*, 3004.

(9) Morosin, B. *Acta Crystallogr., Sect. B: Struct. Crystallogr. Cryst. Chem.* **1970**, *B26*, 1203.

(10) Bonner, J. C.; Friedberg, S. A.; Kobayashi, H.; Meier, D.; Blöte, H. W. *J. Phys. Rev. B: Condens. Matter* **1983**, *27*, 248.

(11) Ferrari, M. B.; Capacchi, L. C.; Fava, G. G.; Nardelli, M. *J. Cryst. Mol. Struct.* **1972**, *2*, 291.

(12) Tomlinson, A. A. G.; Hathaway, B. J. *J. Chem. Soc. A* **1968**, 2578.

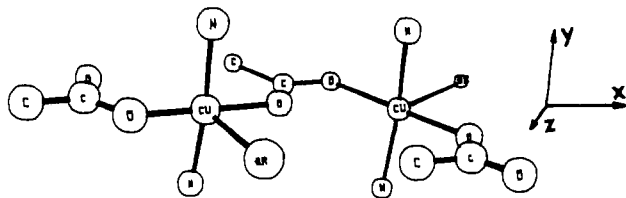


Figure 1. Perspective view of the chain in $[\text{Cu}(\text{NH}_3)_2(\text{CH}_3\text{COO})\text{Br}]$.

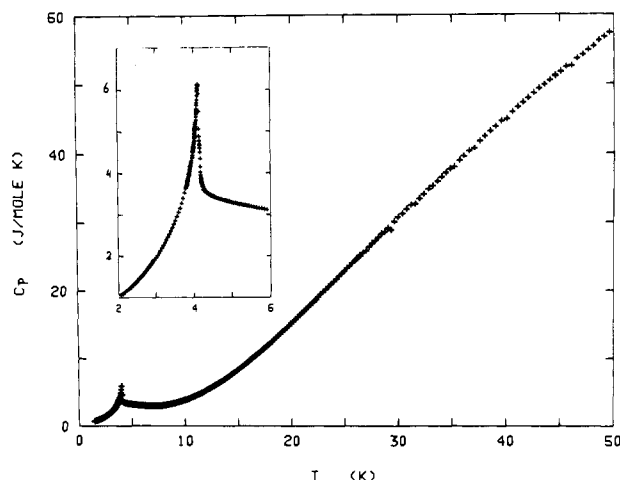


Figure 2. Heat capacity of $[\text{Cu}(\text{NH}_3)_2(\text{CH}_3\text{COO})\text{Br}]$ vs. temperature. The λ -anomaly at $T = 4.146$ K is associated with the 3-D ordering.

and dried in vacuo. Anal. Calcd. for $\text{C}_2\text{H}_9\text{N}_2\text{O}_2\text{BrCu}$: C, 10.15; H, 3.84; N, 11.84; Br, 33.78; Cu, 26.86. Found: C, 10.12; H, 3.85; N, 11.78; Br, 33.06; Cu, 27.5. A specimen consisting of 30.75 g (0.13 mol) of small crystals (average dimensions $3 \times 2 \times 2$ mm) was sealed inside a vacuum calorimeter of conventional design, which was equipped with a temperature-controlled heat screen to enable accurate measurements at higher temperatures. The calorimeter assembly was immersed in liquid ^4He . Temperature readings were obtained from a calibrated germanium thermometer, which was measured with a four-wire ac resistance bridge operating at 33 Hz. The magnetic data were obtained in two stages, with a Faraday type magnetometer equipped with a continuous-flow ^4He cryostat above 4.2 K and with a mutual-inductance bridge below that temperature.¹³ The diamagnetic correction was estimated⁶ as -117×10^{-6} emu mol^{-1} . The independence of the magnetic susceptibility vs. the magnetic field (up to 1.2 T) was checked at both room temperature and 4.2 K. The X-band EPR spectra were recorded with a Bruker ER 200 spectrometer equipped with a continuous-flow cryostat.

Results

The experimental specific heat data between 1.5 and 50 K are shown in Figure 2. The data are corrected for the heat capacity of the empty sample holder, which was measured in a separate run, and varied from 15% of the total at 1.5 K to 45% at 50 K. The λ -anomaly at 4.146 K that is shown in the insert in more detail is associated with the onset of 3-D long-range order. Inspection of Figure 2 reveals a significant magnetic contribution in the paramagnetic region up to about 15 K, suggesting low-dimensional magnetic behavior. The degree of low dimensionality may be estimated from the critical entropy, i.e., the fraction of magnetic entropy removed below the ordering temperature. This fraction was estimated as follows. Since at low temperatures the lattice heat capacity C_L is almost negligible, the magnetic entropy gain for $1.5 \text{ K} < T < T_c$ was evaluated by numerical integration of C/T , whereas below 1.5 K the heat capacity was approximated by the relation $C = aT^b$. The parameters a and b were obtained by a fit to the data for $1.5 < T < 2.5$ K. The critical entropy was found to amount to 42% of the total entropy content $R \ln$

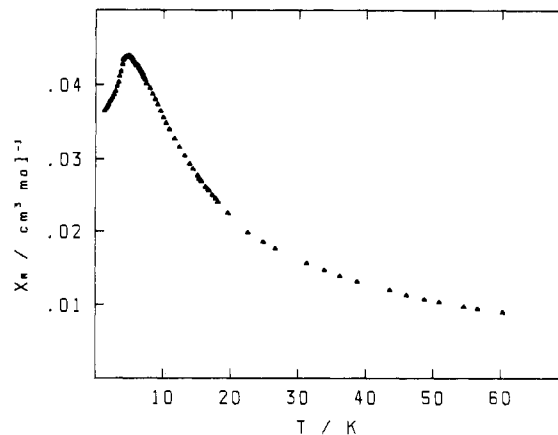


Figure 3. Temperature dependence of the molar magnetic susceptibility of $[\text{Cu}(\text{NH}_3)_2(\text{CH}_3\text{COO})\text{Br}]$.

2 of a spin $S = 1/2$ system. Given the rather large contribution of the extrapolated region below 1.5 K, the relative accuracy of this estimate is about 10%.

The thermal variation of the molar magnetic susceptibility of a polycrystalline sample is shown in Figure 3. Data are available only on the polycrystalline material. Down to 10 K, χ_M follows a Curie-Weiss law with a Curie constant of 0.455 emu K mol^{-1} and $\theta = -6.7$ K. Below 10 K, χ_M deviates from this law and exhibits a maximum around 4.9 K. The ordering temperature obtained from these data is 4.2 K, which is in satisfactory agreement with the value obtained from the more precise specific heat results.

The X-band EPR spectra were recorded on both polycrystalline samples and single crystals. They are typical of a copper(II) ion in rhombic symmetry. The single-crystal EPR spectra show exchange narrowing ($\Delta H_{pp} \sim 10$ G) and angular dependence of band shape and width, with a rapid broadening of the bands when T_c is approached. At 300 K, the g tensor is defined by $g_a = 2.128$ along the chain axis, $g_b = 2.056$ along the N-Cu-N direction, and $g_c = 2.222$.

Discussion

Let us start the discussion with the magnetic susceptibility. The first evidence is that the interaction between the copper(II) ions through the acetato bridge is much weaker than in the hydrated copper acetate. The second interesting point is that, in spite of the structural features, the magnetic properties are not those of a quasi-1-D system of equally spaced $S = 1/2$ spins. Indeed, χ_M does not follow the Bonner-Fisher model¹⁴ for isolated $S = 1/2$ chains. In particular, the magnetic behavior in the range around 4 K does not correspond to the broad maximum characteristic of such systems. On the other hand, the susceptibility data can be fit when a rather large molecular field correction in the Bonner-Fisher model is introduced. The parameters were then found as $g = 2.2$, $J/k = -4.3$ K, and $zJ'/k = 1.9$ K with an exchange Hamiltonian defined as

$$H = \sum_i (-2J\hat{S}_i\hat{S}_{i+1} - 2zJ'\langle S_{iz} \rangle S_{iz} + g\mu_B\hat{S}_i\vec{H})$$

Below 10 K, this model is found to be no longer valid.

Given the chainlike structure of the substance and the apparent low-dimensional characteristics, we tried to describe the magnetic heat capacity C_M above the ordering temperature by an $S = 1/2$ linear-chain model, assuming that at higher temperatures the interchain interactions J' have only a very small effect on C_M . Given the value of the experimental data in the temperature region just above T_c (≈ 3 J/(mol K)) and the expected largely isotropic exchange interaction in cupric compounds, the magnetic contribution was approximated by the $S = 1/2$ Bonner-Fisher model.¹⁴ The lattice contribution C_L was represented by a pseudo-1-D quasi-elastic model,¹⁵ which has been demonstrated¹⁶ to be ap-

(13) McElearney, J. N.; Losee, D. B.; Merchant, S.; Carlin, R. L. *Phys. Rev. B: Solid State* 1973, 7, 3314. Bhatia, S. N.; Carlin, R. L.; Filho, A. P. *Physica B+C (Amsterdam)* 1977, 92B+C, 330. van der Bilt, A.; Jong, K. O.; Carlin, R. L.; de Jongh, L. J. *Phys. Rev. B: Condens. Matter* 1980, 22, 1259.

(14) Bonner, J. C.; Fisher, M. E. *Phys. Rev. A* 1964, 136, 640.

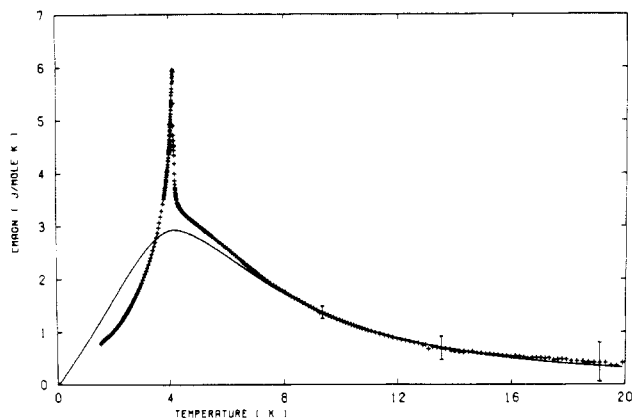


Figure 4. Magnetic heat capacity of $[\text{Cu}(\text{NH}_3)_2(\text{CH}_3\text{COO})\text{Br}]$. Crosses represent experimental data minus the inferred lattice contribution, C_L . The drawn curve represents the heat capacity of an $S = 1/2$ Bonner-Fisher chain with $J/k = -4.3$ K.

appropriate for systems having a significant amount of elastic anisotropy.

Simultaneous fits of C_L and C_M to the experimental data above T_c resulted in a satisfactory description of the data for $T > 8$ K and yielded an intrachain exchange interaction $J/k = -4.3 \pm 0.4$ K. The uncertainty in the value of J/k is mainly caused by correlations between the parameter J/k and the three parameters that were used to fit C_L and was estimated by performing fits to the data in different temperature regions. The accuracy of the description between 8 and 50 K was comparable to the scatter in the experimental data (0.5%).

Preliminary but unsatisfactory fits of the magnetic specific heat to an alternating-linear-chain model revealed a very large correlation between the resulting values of J_1 and J_2 , mainly because the temperature region in which the data can be reasonably described by a 1-D model is drastically limited by the high value of T_c and because there is a lack of independent experimental information about the lattice heat capacity.

The resulting experimental magnetic heat capacity $C_M(\text{exptl}) = C_p(\text{exptl}) - C_L(\text{calcd})$ is plotted in Figure 4 for $T < 20$ K. The error bars reflect the uncertainty in $C_L(\text{calcd})$. The agreement for $T > 8$ K is obviously very good. For $T_c < T < 8$ K, however, the data are significantly higher than the theoretical estimate, which may be attributed to two different effects. First, the interchain interactions in the present compound are rather large, as is obvious from the relatively high value of the critical entropy compared to other quasi-1-D antiferromagnetic cupric systems.¹⁷ This is corroborated by an estimate of the interchain coupling by a Green's function method given by Oguchi,¹⁸ which yields $J'/J \approx 0.1$. Secondly, the description of the magnetic interactions by a purely isotropic Heisenberg model may be somewhat crude, which is also indicated by the total experimental magnetic entropy gain. This is found to be about 8% lower than the value $R \ln 2$ expected for an $S = 1/2$ system. This discrepancy is far outside the experimental error (<1%). In judging these figures, however, one should note that the uncertainty in the extrapolated fraction below 1.5 K is rather large. An accurate estimate of the anisotropy in the present compound from the available data is not possible, hence single-crystal susceptibility measurements may be necessary to clarify the details of the observed behavior.

The investigation of the thermal properties of the compound shows that the magnetic dimensionality of $[\text{Cu}(\text{NH}_3)_2(\text{CH}_3\text{COO})\text{Br}]$ does not follow its structural dimensionality. In fact, intra- and interchain interactions are of the same order of magnitude

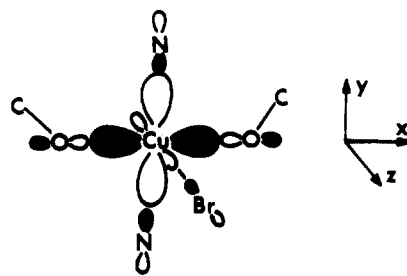


Figure 5. Magnetic orbital centered on copper(II) ion in $[\text{Cu}(\text{NH}_3)_2(\text{CH}_3\text{COO})\text{Br}]$, as obtained by an extended-Hückel calculation.

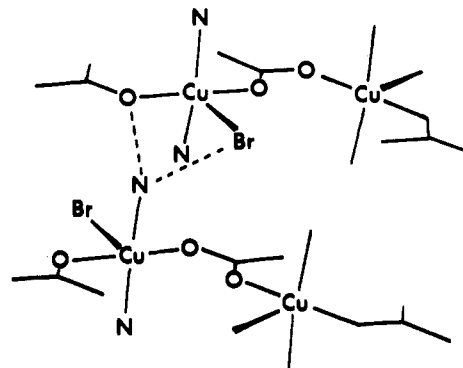
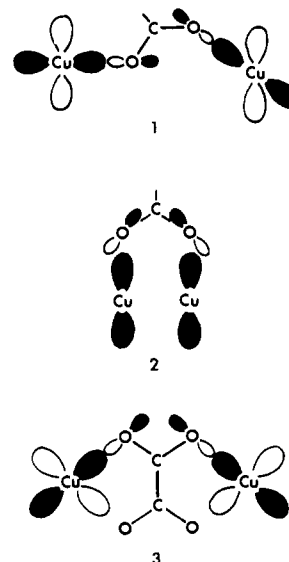


Figure 6. Hydrogen-bonding network in $[\text{Cu}(\text{NH}_3)_2(\text{CH}_3\text{COO})\text{Br}]$.

Chart I



and the 3-D ordering occurs at a relatively high temperature. The problem at hand is then this: Is it possible to rationalize this peculiar behavior on an orbital basis? The unpaired electron around each metal center is described by a magnetic orbital of $x^2 - y^2$ type pointing toward the oxygen and nitrogen atoms of the basal plane with some admixture of a z^2 type orbital pointing toward the bromine atom in apical position,⁷ as schematized in Figure 5. Along the chain, the magnitude of the antiferromagnetic interaction is governed by the overlap of two magnetic orbitals of this kind centered on nearest-neighbor copper(II) ions.¹⁹ Owing to the symmetry of the $\text{Cu}_1\text{-O}_1\text{-C}(\text{CH}_3)\text{-O}_2\text{-Cu}_2$ bridging network, the contributions of the 2p orbitals O_1 and O_2 belonging to the magnetic orbitals centered on Cu_1 and Cu_2 respectively are unfavorably oriented to give a strong overlap. This situation, 1, shown in Chart I contrasts with situations 2 and 3 encountered in hydrated copper(II) acetate and planar oxalato-bridged copper(II) systems.^{7,8}

- (15) Kopinga, K.; van der Leeden, P.; de Jonge, W. J. M. *Phys. Rev. B: Solid State* **1976**, *14*, 1519.
 (16) de Jonge, W. J. M.; Swüste, C. H. W.; Kopinga, K.; Takeda, K. *Phys. Rev. B: Solid State* **1975**, *12*, 5858.
 (17) Takeda, K.; Yoshino, Y.; Matsumoto, K.; Haseda, T. *J. Phys. Soc. Jpn.* **1980**, *49*, 162.
 (18) Oguchi, T. *Phys. Rev. A* **1964**, *133*, 1098.

- (19) Girerd, J. J.; Charlot, M. F.; Kahn, O. *Mol. Phys.* **1977**, *34*, 1063.

As for the interaction between chains, it can be associated with the hydrogen-bonding networks along the two pathways Cu-N(H₃)-O-Cu with $d_{\text{N-O}} = 3.048 \text{ \AA}$ and $d_{\text{Cu-Cu}} = 5.22 \text{ \AA}$, and Cu-N(H₃)-Br-Cu with $d_{\text{N-Br}} = 3.156 \text{ \AA}$ and $d_{\text{Cu-Cu}} = 5.22 \text{ \AA}$. These pathways are represented in Figure 6. They involve nitrogen, oxygen, or bromine atoms directly bound to copper atoms, on which the spin density is partially delocalized, so that they may efficiently transmit the interaction between metal atoms belonging to different chains and separated by 5.22 Å. Therefore, the interchain interaction is far from being negligible and is actually of the same order of magnitude as the intrachain interaction

through the carboxylate bridge, which explains the high temperature of 3-D antiferromagnetic ordering.

Acknowledgment. The Solid State Chemistry program of the Division of Materials Research of the National Science Foundation, under Grants DMR-7906119 and DMR-8211237, supported the contribution by R.L.C. Some of the susceptibility measurements were carried out by D. W. Carnegie, Jr., and P. Eenshuistra helped to collect the specific heat data.

Registry No. [Cu(NH₃)₂(CH₃COO)Br], 50589-00-9.

Contribution from the Department of Chemistry, The University, Southampton SO9 5NH, U.K., and Daresbury Laboratory, Daresbury, Warrington WA4 4AD, U.K.

Coordination Chemistry of Higher Oxidation States. 19.[†] Synthesis and Properties of Diposphine and Diarsine Complexes of Iron(IV) and Iron K-Edge EXAFS Data on [Fe(*o*-C₆H₄(PMe₂)₂)₂Cl₂]ⁿ⁺[BF₄]_n (*n* = 0-2)

Stephen K. Harbron,[†] Simon J. Higgins,[†] William Levason,^{*†} Martinus C. Feiters,[§] and Andrew T. Steel[§]

Received August 26, 1985

Pure samples of the iron(IV) complexes [Fe(L-L)₂X₂][BF₄]₂ (L-L = *o*-C₆H₄(PMe₂)₂, *o*-C₆H₄(PMe₂)(AsMe₂), *o*-C₆H₄(AsMe₂)₂, X = Cl, Br; L-L = Me₂PCH₂CH₂PMe₂, X = Cl) have been isolated, and the corresponding complexes [Fe(*o*-C₆H₄(PMe₂)₂)₂X₂]²⁺ (X = Cl, Br) and [Fe(Me₂PCH₂CH₂PMe₂)₂Br₂]²⁺ have been obtained in solution. Magnetochemical, IR, and electronic spectroscopic data are reported, and the Fe^{II} ↔ Fe^{III} ↔ Fe^{IV} redox potentials have been studied as a function of L-L and X by cyclic voltammetry. Iron K-edge EXAFS data on the title complexes have been analyzed to provide the iron-ligand bond lengths (Å) for [Fe(*o*-C₆H₄(PMe₂)₂)₂Cl₂]ⁿ⁺ (*n* = 0, Fe-Cl = 2.35, Fe-P = 2.23; *n* = +1, Fe-P and Fe-Cl = 2.245 (av); *n* = 2, Fe-Cl = 2.16, Fe-P = 2.33), and the trends in these values are discussed.

Introduction

The chemistry of iron(IV) is not extensive, but this oxidation state has attracted considerable attention due to its occurrence in oxidized iron porphyrins. The formulation of the oxidation products of iron(III) porphyrins has been a controversial topic, but recent investigations have provided good evidence (especially from ⁵⁷Fe Mössbauer spectroscopy) for both iron(III) porphyrin π-cation radicals¹⁻³ and iron(IV) porphyrins⁴⁻⁷ and very recently for a stable iron(IV) π-radical porphyrin.⁸ Among the "simple" iron(IV) complexes are the oxometalates Na₄FeO₄, Ba₂FeO₄,⁹ dithio-¹⁰⁻¹² and diselenocarbamates¹³ [Fe(Z₂CNR₂)₃]⁺ (Z = S, Se), and 1,1-dithiolates [Fe(S₂CCR₂)₃]²⁻.¹⁴ Iron(IV) complexes with neutral ligands are limited to unstable [Fe(*o*-C₆H₄(AsMe₂)₂)₂X₂][BF₄]₂ (X = Cl, Br)^{15,16} and [Fe(*o*-C₆H₄(PMe₂)₂)₂Cl₂][ReO₄]₂,¹⁷ and for these the magnetic properties are disputed and no structural data are available.

We have recently shown^{18,19} that structural data can be obtained for similarly unstable nickel(IV) diposphines by metal K-edge EXAFS, and here we report a similar study of the iron(IV) complexes. A preliminary account of this work has appeared.²⁰

Results

The iron(IV) complexes [Fe(L-L)₂X₂][BF₄]₂ (L-L = *o*-C₆H₄(PMe₂)₂, *o*-C₆H₄(AsMe₂)₂, *o*-C₆H₄(PMe₂)(AsMe₂); X = Cl, Br) (Table I) were obtained by nitric acid oxidation of the iron(III) analogues, followed by precipitation with HBF₄. Since purity is often markedly dependent upon the counterion (cf. ref 19), other ions including ClO₄⁻, ReO₄⁻, PF₆⁻, and CF₃SO₃⁻ were considered. (The isolation of [FeCl₄]⁻ salts has been reported,¹⁵ but the presence of a second iron center makes them unsuitable for magnetochemical and EXAFS studies.) The perchlorates are highly explosive,¹⁵ the perrhenates are prone to introduce nit-

rogenous impurities, and while PF₆⁻ readily gave precipitates of the iron(IV) complexes, these had poor analyses and the IR spectra showed other fluorophosphate ions to be present (mainly PO₂F₂⁻). Trifluoromethanesulfonic acid did not precipitate the complexes from solution, and hence the BF₄⁻ salts were used in this study. Although these are reportedly¹⁶ hygroscopic, we found that *thoroughly dried* pure samples absorbed water only slowly. The syntheses are described in the Experimental Section, purity being

- (1) Boersma, A. D.; Goff, H. M. *Inorg. Chem.* **1984**, *23*, 1671 and references therein.
- (2) Phillippi, M. A.; Goff, H. M. *J. Am. Chem. Soc.* **1982**, *104*, 6026.
- (3) Shimomura, E. T.; Phillippi, M. A.; Goff, H. M.; Scholz, W. F.; Reed, C. A. *J. Am. Chem. Soc.* **1981**, *103*, 6778.
- (4) Kadish, K. M.; Rhodes, R. K.; Bottomley, L. A.; Goff, H. M. *Inorg. Chem.* **1981**, *20*, 3195.
- (5) English, D. R.; Hendrickson, D. N.; Suslick, K. S. *Inorg. Chem.* **1983**, *22*, 367.
- (6) Hiller, W.; Strahle, J.; Datz, A.; Hanack, M.; Hatfield, W. E.; ter Haar, L. M.; Gutlich, P. *J. Am. Chem. Soc.* **1984**, *106*, 329.
- (7) Grove, J. T.; Quinn, R.; McMurray, T. J.; Nakamura, M.; Lang, G.; Boso, B. *J. Am. Chem. Soc.* **1985**, *107*, 354.
- (8) English, D. R.; Hendrickson, D. N.; Suslick, K. S. *Inorg. Chem.* **1985**, *24*, 123.
- (9) Scholder, R. *Z. Elektrochem.* **1952**, *56*, 879. Scholder, R.; Bunsen, H. V.; Zeiss, W. *Z. Anorg. Allg. Chem.* **1956**, *283*, 330.
- (10) Pasek, E. A.; Straub, D. K. *Inorg. Chem.* **1972**, *11*, 259.
- (11) Chant, R.; Hendrickson, A. R.; Martin, R. L.; Rohde, N. M. *Inorg. Chem.* **1975**, *14*, 1814.
- (12) Martin, R. L.; Rohde, N. M.; Robertson, G. B.; Taylor, D. *J. Am. Chem. Soc.* **1974**, *96*, 3647.
- (13) Deplano, P.; Trogu, E. F.; Bigoli, F.; Laporate, E.; Pellighelli, M. A.; Perry, D. L.; Saxon, R. J.; Wilson, L. *J. Chem. Soc., Dalton Trans.* **1983**, 25.
- (14) Hollander, F. J.; Pedelty, R.; Coucouvanis, D. *J. Am. Chem. Soc.* **1974**, *96*, 4032.
- (15) Nyholm, R. S.; Parish, R. V. *Chem. Ind. (London)* **1956**, 470.
- (16) Hazeldean, G. S. F.; Nyholm, R. S.; Parish, R. V. *J. Chem. Soc. A* **1966**, 162.
- (17) Warren, L. F.; Bennett, M. A. *Inorg. Chem.* **1976**, *15*, 3126.
- (18) Steel, A. T.; Feiters, M. C.; Garner, C. D.; Hasnain, S. S.; Higgins, S. J.; Levason, W. *J. Chem. Soc., Chem. Commun.* **1985**, 484.
- (19) Higgins, S. J.; Levason, W.; Feiters, M. C.; Steel, A. T. *J. Chem. Soc., Dalton Trans.* **1986**, 317.
- (20) Harbron, S. K.; Higgins, S. J.; Levason, W.; Feiters, M. C.; Steel, A. T.; Garner, C. D.; Hasnain, S. S. *J. Am. Chem. Soc.* **1986**, *108*, 526.

[†] Part 18: Hope, E. G.; Levason, W.; Webster, M.; Murray, S. G. *J. Chem. Soc., Dalton Trans.*, in press.

[‡] The University, Southampton.

[§] Daresbury Laboratory.